98

Determination of optimal parameters for a hydraulic power take-off unit of a wave energy converter in regular waves

C J Cargo*, A R Plummer, A J Hillis, and M Schlotter

Centre for Power Transmission and Motion Control, University of Bath, Bath, UK

The manuscript was received on 10 December 2010 and was accepted after revision for publication on 31 March 2011.

DOI: 10.1177/0957650911407818

Abstract: Wave energy has the potential to be a major provider of renewable energy, especially in the UK. However, there is the major problem of producing efficient devices for a wide variety of sites with different operating conditions. This article addresses the time domain modelling of a heaving point absorber connected to a hydraulic power take-off (PTO) unit in regular waves. Two cases for the hydraulic PTO unit are considered: an ideal model and a model containing losses. Component losses are included to give a more accurate prediction of the maximum power production and to discover if the parameters to optimize the device change when losses are included. The findings show that both cases are optimized by varying the size of the hydraulic motor and the optimal size is only dependent on wave period and the trend is the same for both cases. Results also showed that to maximize the power produced for both cases, there is an optimal force that the unit produces, which can be derived from theory. Finally, power reduction as a result of the hydraulic losses is also observed with efficiencies reducing at larger wave heights.

Keywords: wave energy, hydraulic PTO, efficiency, power optimization

1 INTRODUCTION

It is estimated that the worldwide power available from sea waves is 2 TW, which is comparable to the magnitude of the world's electricity generation [1]. To extract this power, a wave energy converter (WEC) must resist wave forces in a carefully controlled way. An extensive review of the many methods proposed to perform this is available in Drew *et al.* [2]. The most common approach is to use a hydraulic power take-off (PTO) unit due to its high power density and robustness, which is an obvious advantage for offshore operations, where maintenance costs can be very high [1, 3]. A direct drive electric generator is an alternative design for the PTO unit but the drawback is that the generator will encounter lower speeds than typical high-speed rotary generators,

email: cjc25@bath.ac.uk

which means that there is a requirement for a physically larger machine [4]. Both types of system, however, will require a grid connection as demonstrated in Rahm *et al.* [5]. A significant problem is the optimization of hydraulic PTO devices in sea states of varying wave amplitude, direction, and frequency. Sub-optimal configuration can result in very inefficient energy conversion [6], so understanding the design trade-offs is the key to the success of the technology.

Previous work has focused on developing control methods for point absorbers to maximize the energy absorbed. Falcão [7] used a simplified hydraulic PTO unit connected to a point absorber to develop an algorithm to optimize the converter. The algorithm was shown to be weakly dependent on wave period and independent of wave height when simulated in real sea conditions and to produce power levels similar to a fully linear PTO unit. This work was continued in Falcão [8] to include a strategy for phase control by latching to increase the absorbed power

^{*}Corresponding author: Centre for Power Transmission and Motion Control, University of Bath, Claverton Down, Bath BA2 7AY, UK.

further. In Babarit et al. [9] three different latching control strategies are compared to show their effectiveness in different sea states with all three strategies giving a considerably increased efficiency in irregular waves. In Yavuz et al. [10] work focuses on assessing the performance of a tuneable point absorber by trying to fulfil the condition of resonance by varying the PTO characteristics. Results showed a maximum power capture of 50 per cent of the rated power in regular waves. This work was continued in Yavuz et al. [11] with irregular waves to show that power capture can be maximized by continuously tuning the natural frequency of the device to the incoming wave frequency. More recently, in Folley and Whittaker [12], a new control method called active bipolar damping or declutching is proposed which tries to shift the buoy's velocity so it is in phase with the wave force. When compared theoretically to other methods, it shows a higher power capture than optimum linear damping without the requirement of reactive energy storage. This control method has been investigated in Babarit et al. [13] using a hydraulic PTO and compared to a control method which tries to mimic the continuous behaviour of a viscous damper. Results show greater power levels from the declutching control method with the added advantage of requiring a less complex system.

Most of these investigations use linearized models and do not consider real hydraulic circuits and components in their investigations. This study uses the simulation of a combined hydrodynamic and realistic PTO unit model to investigate and optimize the performance in a variety of sea conditions by sizing certain key hydraulic components correctly. Section 2 describes the modelling and optimization of a linear PTO unit (i.e. a viscous damper) in the frequency domain. Section 3 covers the time domain modelling of an ideal hydraulic PTO unit. Section 4 presents a realistic PTO unit with losses. Finally, in section 5, the conclusions are presented.

2 MODELLING AND OPTIMIZATION WITH A LINEAR PTO

The device, illustrated in Fig. 1, comprises a single heaving buoy which is linked to the sea-bed or a reaction plate by the PTO unit. Varying the force produced by the PTO unit allows control strategies to be implemented, effectively varying the PTO impedance to optimize the power absorbed. In this study, all other degrees of freedom are neglected and regular monochromatic waves are used as an input. Regular waves are an idealistic approach but it is a natural starting point for the study, as shown in references [8], [9], [12], and [13].

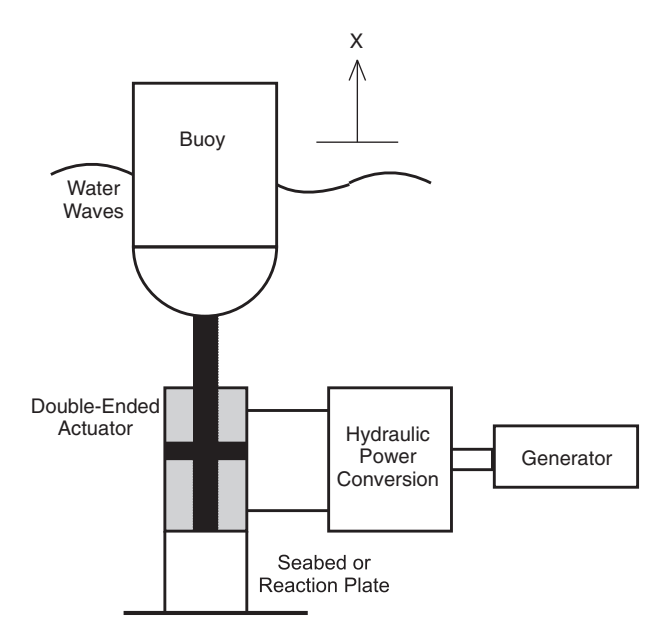


Fig. 1 Schematic of the WEC

The buoy is assumed to be a vertical cylindrical body with an extended hemisphere at its lower end to reduce viscous drag. There are no limitations on the amplitude of motion of the buoy. The buoy dimensions chosen are a mass of 39 tonnes, a radius of 2 m, and a draft of 4 m, as these are similar to dimensions of devices currently being prototyped.

Assuming an incompressible fluid with zero viscous losses, linear wave theory can be used to solve the governing hydrodynamic equations. The equation for the buoy motion is

$$m\ddot{x} = f_{\rm h}(t) + f_{\rm m}(t) \tag{1}$$

where m is the mass of the buoy, \ddot{x} the buoy's acceleration, $f_{\rm h}(t)$ the vertical component of the total wave force, and $f_{\rm m}(t)$ the vertical component of the mechanical force. The wave force can be further decomposed as follows [14]

$$f_{\rm h}(t) = f_{\rm e}(t) + f_{\rm r}(t) + f_{\rm hs}(t)$$
 (2)

where $f_{\rm e}(t)$, the excitation force, is the force produced by the incident waves on an otherwise fixed body. The radiation force, $f_{\rm r}(t)$, is the force produced by an oscillating body creating waves on an otherwise calm sea, and $f_{\rm hs}(t)$ is the linearized form of the hydrostatic force. With these assumptions, the excitation force is proportional to the incident wave amplitude [7], so

$$f_{\rm e}(t) = \Gamma(\omega) \frac{H}{2} \sin \omega t$$
 (3)

where $\Gamma(\omega)$ is the excitation force coefficient which is dependent on the body's shape and the wave frequency (ω) [14] and H the wave height. The radiation force can be decomposed into components in

phase with the buoy's acceleration and velocity such that

$$f_{\rm r}(t) = -A(\omega)\ddot{x} - B(\omega)\dot{x} \tag{4}$$

The coefficients $A(\omega)$ and $B(\omega)$ are the added mass and radiation damping coefficients, respectively, and are dependent on the buoy shape and wave frequency [14, 15]. The hydrostatic force is given by

$$f_{\rm hs}(t) = -\rho g S x \tag{5}$$

where ρ is the water density, g the gravitational constant, and S the buoy cross-sectional area in the x-direction.

The mechanical forces acting on the WEC comprise the vertical component of the force applied on the buoy by the PTO unit and the mooring force. Assuming the effect of the mooring force on the buoy is sufficiently small to be neglected and the PTO force to be a linear function of buoy velocity, the mechanical force becomes

$$f_{\rm m} = -C\dot{x} \tag{6}$$

where C is the damping coefficient. Equation (1) may then be re-written as

$$(m+A)\ddot{x} + (B+C)\dot{x} + (\rho gS)x = f_e(t)$$
 (7)

2.1 Frequency domain analysis

To theoretically determine the criteria for maximum energy absorption, it is useful to use the frequency domain. Taking the Laplace transform of equation (7) gives the following transfer function

$$\frac{X(s)}{F_{e}(s)} = \frac{1}{(m+A)s^{2} + (B+C)s + (\rho gS)}$$
(8)

Transforming into the frequency domain

$$X(j\omega) = \frac{F_{\rm e}(j\omega)}{-\omega^2(m+A) + j\omega(B+C) + \rho gS}$$
 (9)

Equation (9) can be re-written in terms of velocity, *U*, to give

$$U(j\omega) = \frac{F_{\rm e}(j\omega)}{i\omega(m+A) + (B+C) + (\rho gS/i\omega)}$$
(10)

Looking at the transfer of power in the system, the time averaged useful power absorbed by the PTO is given by

$$\bar{P} = \frac{1}{2}C|U(j\omega)|^2 \tag{11}$$

Substituting for $U(j\omega)$ using equation (10)

$$\bar{P} = \frac{\frac{C}{2} F_{e}(\omega)^{2}}{(B+C)^{2} + (\omega(m+A) - (\rho gS/\omega))^{2}}$$
(12)

There is an optimum condition to maximize the energy conversion. The condition for the optimum PTO damping rate, $C_{\rm opt}$, can be obtained from $\frac{\partial \bar{P}}{\partial C} = 0$. This gives

$$C_{\text{opt}} = \sqrt{\left(B^2 + \left(\omega(m+A) - \frac{\rho gS}{\omega}\right)^2\right)}$$
 (13)

Figure 2 shows that $C_{\rm opt}$ varies approximately linearly with the period of the incoming wave in this frequency range of interest and equation (13) indicates that $C_{\rm opt}$ is independent of wave height. There is also an optimum buoy velocity amplitude, $U_{\rm opt}$, to maximize the energy absorption which is obtained by rearranging equations (3) and (9) and using the optimum PTO damping rate $C_{\rm opt}$. This gives

$$U_{\text{opt}} = \frac{\Gamma(\omega)(H/2)}{\sqrt{(C_{\text{opt}} + B)^2 + (\omega(m+A) - (\rho gS/\omega))^2}}$$
(14)

Figure 2 shows that the relationship between $U_{\rm opt}$ and the wave period is non-linear. However, equation (14) indicates that there is a linear relationship between $U_{\rm opt}$ and wave height. These two optimum conditions can then be combined to give the optimum PTO force amplitude $\Phi_{\rm opt}$, which is given by

$$\Phi_{\rm opt} = C_{\rm opt} U_{\rm opt} \tag{15}$$

Figure 3 shows that, as expected, Φ_{opt} does not vary linearly with wave period. However, it does vary

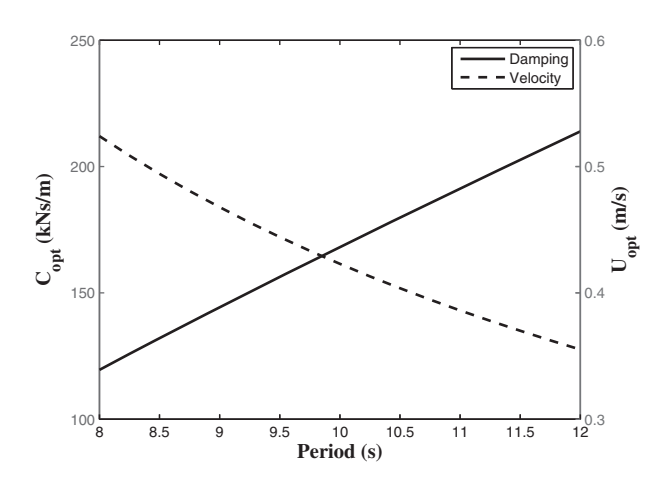


Fig. 2 Optimum damping coefficient and buoy velocity amplitude against wave period for a wave height of 2 m

linearly with wave height, and the values shown are for a wave height of 2 m.

3 TIME DOMAIN HYDRODYNAMIC MODELLING

Real hydraulic circuits are non-linear due to valve switching, pressure losses, and many other component characteristics. Therefore, analysis of realistic systems must be conducted in the time domain. Cummins [16] developed an approach for investigating ship response to sea waves, which has been widely applied and accepted when investigating WECs. With this approach, the equation of motion takes the form

$$(m+A_{\infty})\ddot{x}(t) + \rho gSx(t) + \int_{-\infty}^{t} L(t-\tau)\dot{x}d\tau$$

= $f_{e}(t) + f_{m}(x,\dot{x},t)$ (16)

where A_{∞} is the limiting value of the added mass term, i.e. $A(\omega)$ for $\omega = \infty$. L(t) is a function representing the memory effect of the radiation force, which is dependent on the history of the buoy motion. This memory effect decays with time, which implies that the force produced by the buoy motion no longer affects the current movement of the buoy after a certain time. L(t) is given by the sine transform of the radiation damping coefficient $B(\omega)$ [14] such that

$$L(t) = \frac{2}{\pi} \int_0^\infty \frac{B(\omega)}{\omega} \sin(\omega t) d\omega$$
 (17)

To reduce computation time, this memory function has been approximated by a second-order transfer function with the comparison shown in Fig. 4. The excitation force is calculated in the same manner as previously (equation (3)) and all non-linearities are included in the PTO force acting on the buoy.

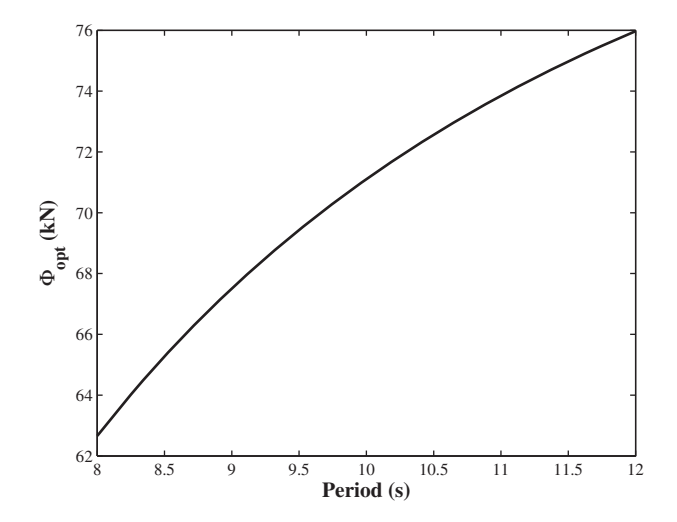


Fig. 3 Optimum PTO force amplitude against wave period for a wave height of 2 m

3.1 Ideal hydraulic PTO

The hydraulic PTO used in this study is shown in Fig. 5. A rigid link between the buoy and the PTO means that the motion of the buoy directly drives a double-acting equal-area hydraulic piston working within a fixed cylinder. This motion drives fluid through a set of four check valves to rectify the flow so that fluid always passes through the hydraulic motor in the same direction (independent of the direction of the buoy motion). A high-pressure accumulator is placed on the inlet to the hydraulic motor and a low-pressure one on the outlet of the hydraulic motor. The pressure difference between the two accumulators drives a variable displacement motor, which is connected to an electrical generator. The accumulators are included to keep an approximate

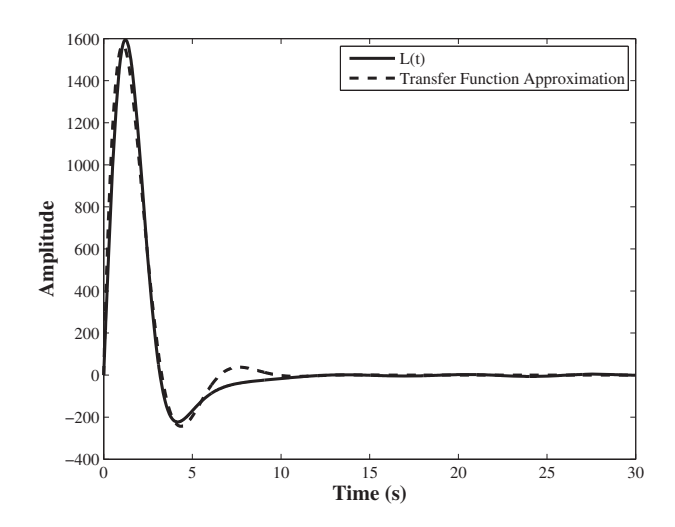


Fig. 4 Memory function comparison

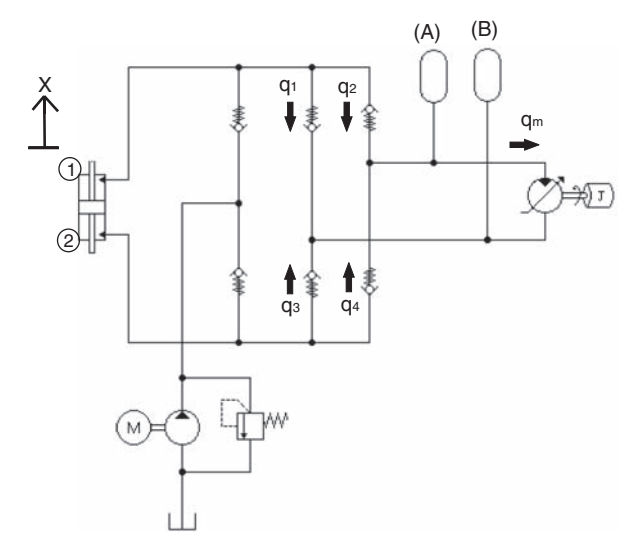


Fig. 5 Hydraulic PTO unit circuit diagram

constant pressure differential across the motor so it spins at an approximate constant speed and therefore, energy is transmitted at approximately a constant rate. The thermodynamic transformations in the accumulators are assumed to be isentropic, which is reasonable considering the cycle time in the device. In this study, the generator is modelled as a simple rotational damper with varying damping coefficient. This means that the resistive torque imposed by the generator can be altered by varying this damping coefficient. A boost pump and pressure relief check valve are required to prevent cavitation and maintain a minimum pressure in the system, which depends on the pressure relief valve setting. In this case, the valve is set to a pressure of 12 bar.

The link between the buoy and the PTO unit is based upon preliminary designs for point absorber devices, which have not yet been proven. However, the fundamental action and design of the PTO unit remains valid and could be applied to many different types of WEC design. In reality, there will be losses throughout the hydraulic circuit such as friction in the piston, pressure losses in the pipes, leakage in the motor, and torque losses due to friction in the motor and generator. These losses will depend on the specific operating conditions in the unit, which are determined by the size of certain components and the constantly changing wave conditions.

As a starting point to help understand the PTO unit, it has been simplified so there are no losses in the circuit. Section 4 will investigate the unit with losses. With these assumptions, the following equations hold true for the hydraulic circuit.

PTO force

$$\Phi = (p_1 - p_2)A_p \tag{18}$$

where p_1 and p_2 are the pressures in the piston chambers and A_p the piston area.

If $sign(\dot{x})$ is positive

$$A_{\rm p}\dot{x} - q_1 - q_2 = \frac{V_1}{R} \frac{\mathrm{d}p_1}{\mathrm{d}t} \tag{19}$$

If $sign(\dot{x})$ is negative

$$A_{\rm p}\dot{x} - q_3 - q_4 = \frac{V_2}{B} \frac{\mathrm{d}p_2}{\mathrm{d}t}$$
 (20)

where V_i is the volume of oil in piston chamber, i=1, 2 and B the bulk modulus of the oil.

$$q_1 = \begin{cases} 0 : p_1 > p_B \\ -K\sqrt{p_B - p_1} : p_B \geqslant p_1 \end{cases}$$
 (21)

$$q_2 = \begin{cases} 0 : p_A > p_1 \\ K\sqrt{p_1 - p_A} : p_1 \ge p_A \end{cases}$$
 (22)

$$q_3 = \begin{cases} 0 : p_2 > p_B \\ -K\sqrt{p_B - p_2} : p_B \ge p_2 \end{cases}$$
 (23)

$$q_4 = \begin{cases} 0 : p_A > p_2 \\ K\sqrt{p_2 - p_A} : p_2 \ge p_A \end{cases}$$
 (24)

K is chosen to be very large so that the pressure drop across each check valve is negligible.

Flow to accumulator 'A'

$$q_{\rm A} = q_2 + q_4 - q_{\rm m} \tag{25}$$

Volume of oil in accumulator 'A'

$$V_{\mathbf{A}}(t) = \int_0^t q_{\mathbf{A}} \mathrm{d}t \tag{26}$$

Flow to accumulator 'B'

$$q_{\rm B} = q_{\rm m} - q_1 - q_3 \tag{27}$$

Volume of oil in accumulator 'B'

$$V_{\rm B}(t) = \int_0^t q_{\rm B} \mathrm{d}t \tag{28}$$

Assuming the compression in the accumulators to be isentropic, the pressure in each accumulator is given by

$$pV^{\gamma} = p_o V_0^{\gamma} \tag{29}$$

where p_o is the pre-charge pressure, V_o the volume of each accumulator, and γ the adiabatic index.

Flow to motor

$$q_{\rm m} = D_{\rm m}\omega_{\rm m} \tag{30}$$

where $D_{\rm m}$ is the motor displacement and $\omega_{\rm m}$ the motor speed.

Rotational acceleration

$$\dot{\omega}_{\rm m} = \frac{D_{\rm m}(p_{\rm A} - p_{\rm B}) - T_{\rm g}}{I} \tag{31}$$

where p_A is the pressure in accumulator 'A', p_B the pressure in accumulator 'B', and J the inertia of the generator.

Generator torque

$$T_{g} = C_{g}\omega_{m} \tag{32}$$

where C_g is the damping coefficient of the generator. Motor torque

$$T_{\rm m} = (p_{\rm A} - p_{\rm B})D_{\rm m} \tag{33}$$

Mechanical power produced by the PTO

$$P_{\rm m} = T_{\rm m}\omega_{\rm m} \tag{34}$$

Table 1 presents the values of the parameters which remained constant in this investigation. These values are not based on any specific design but are a representation of suitable sizing for the buoy size. In this idealized case, the effect of the boost pump is negligible.

3.2 PTO and buoy behaviour

How the PTO unit behaves during one cycle of the buoy motion will now be described. This will first help to determine whether the unit can be compared to the case of a simple viscous damper investigated before. Second, it will help to determine possible ways in which the unit can be optimized.

It is clear from Fig. 6 that the previous assumption of sinusoidal motion made for the case of a viscous damper does not hold true when an ideal hydraulic PTO unit is introduced. It can be seen that the piston is arrested at its endpoints and remains almost stationary for approximately 2 s. The following points,

Table 1 PTO unit component values

Equal area piston	
Area	$0.007\mathrm{m}^2$
Stroke limit	$\pm 2.5\mathrm{m}$
HP gas accumulator 'A'	
Pre-charge pressure	30 bar
Volume	$200\mathrm{L}$
γ	1.4
LP gas accumulator 'B'	
Pre-charge pressure	10 bar
Volume	$200\mathrm{L}$
γ	1.4
Variable displacement motor	
Maximum displacement	0.15 L/rev
Generator	
Damping coefficient	1 Nm/(rad/s)
Inertia	2 kgm ²
Boost pump	J
Displacement	0.05 L/rev

Notes: HP, high pressure; LP, low pressure.

with the help of Figs 6 to 9, will explain the sequence of events which is occurring during the cycle for a wave period of 8 s.

- 1. At time = 390.5 s, the piston approaches its endpoint and the pressure in the piston chamber falls below the accumulator pressure so the check valve closes and there is zero flow to the highpressure accumulator.
- 2. At this point, the piston changes its direction of motion so the high-pressure piston chamber becomes the low-pressure chamber and *visa versa*.
- 3. When the piston is at its endpoints, the wave force is insufficient to overcome the piston force so it is held there for approximately 2 s (time = 390.5–392 s). However, due to the inertia of the buoy, there are still small piston oscillations during this period (Fig. 9).
- 4. When the check valves are closed, this forms two columns of oil in each piston chamber and joining pipeline. As the piston oscillates during this period, it compresses one column of oil and increases the pressure while the other column of oil has a reduction in pressure. This oscillation causes the chamber pressure and piston force oscillations which can be observed in Fig. 8 at time = 391 s.
- 5. The wave force is trying to move the buoy and as it increases, the pressure in one of the chambers increases sufficiently to open the check valve. This causes a small spike in the flow, which can be seen in Fig. 9 at time = 391.5 s.
- 6. When the check valve opens, the pressure reduces and the check valve closes again, resulting in zero

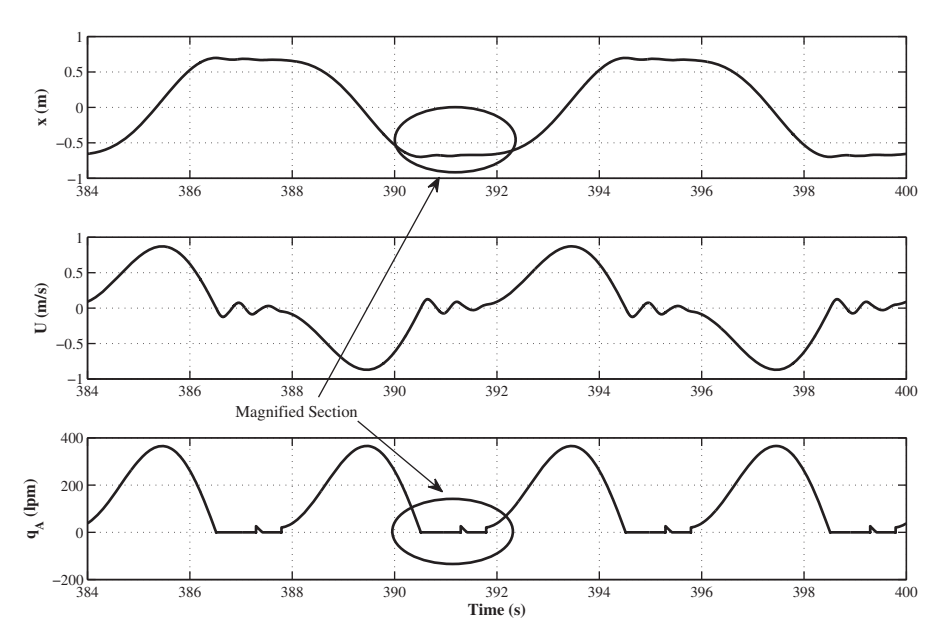


Fig. 6 Piston displacement, velocity, and flow to accumulator 'A' for an ideal hydraulic PTO

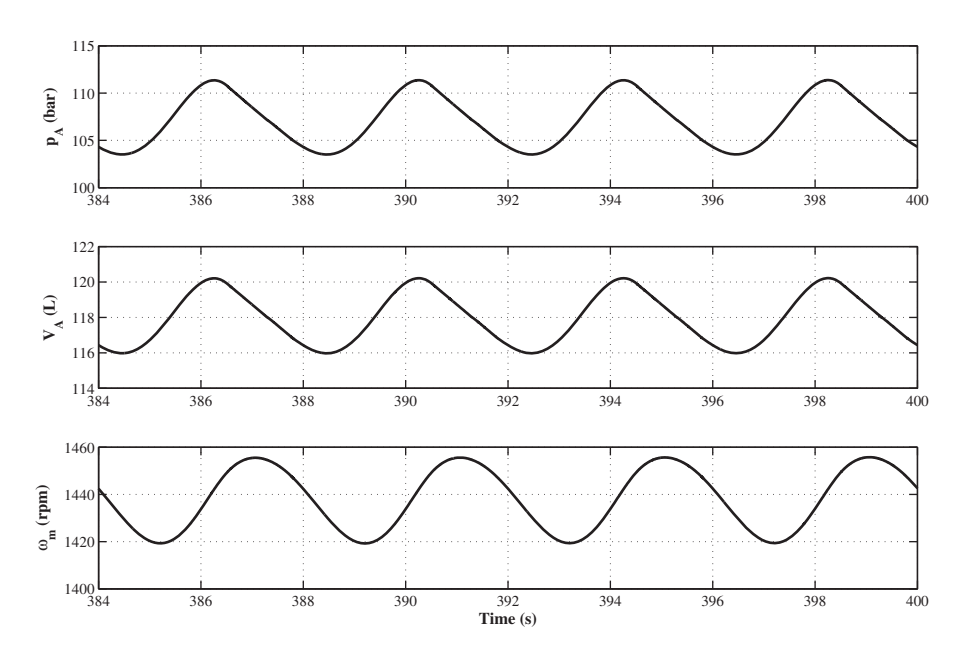


Fig. 7 Accumulator 'A' pressure, volume, and motor speed for an ideal hydraulic PTO

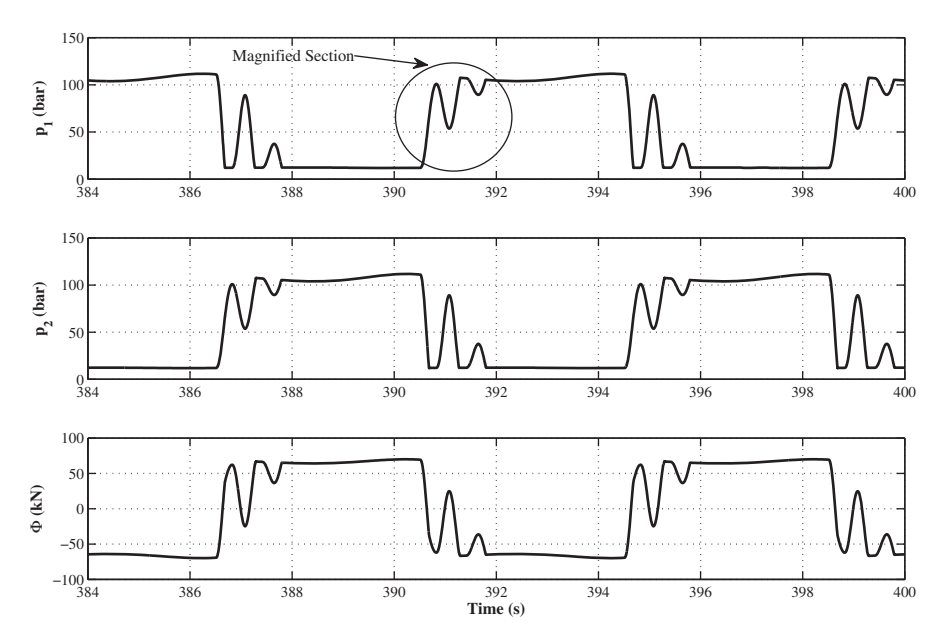


Fig. 8 Piston chamber pressures and piston force for an ideal hydraulic PTO

flow. This occurs because the wave force is still insufficient to overcome the piston force and maintain a piston pressure higher than the accumulator pressure to keep the check valve open.

- 7. At time = 392 s, the wave force becomes greater than the piston force and the pressure in the piston chamber has increased to overcome the pressure in the accumulator. The check valve opens and the piston is now moving freely, which creates flow to the accumulator.
- 8. As the piston velocity increases, the flow increases until the maximum at time = 393.5 s. At the point of maximum piston velocity and flow, the wave

- force becomes less than the piston force again and the piston velocity decreases, which means that the flow begins to reduce.
- 9. Figure 7 indicates that flow from the piston causes the pressure and volume of oil in the accumulator to increase after a short delay.
- 10. The motor speed also increases with the accumulator pressure after a short delay.
- 11. As the pressure in the accumulator increases, the pressure in the piston chamber decreases slightly. At time = 394.5 s, the pressure in the accumulator becomes greater than the piston chamber pressure and the check valve closes.

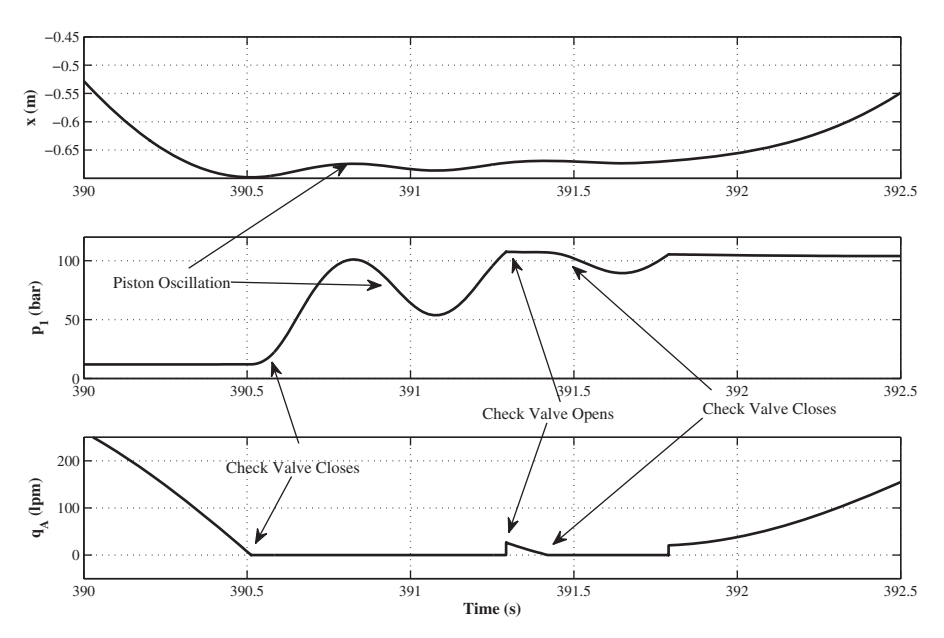


Fig. 9 Magnified section of piston displacement, flow to accumulator 'A', and piston pressure for an ideal hydraulic PTO

- 12. When the check valves are closed and there is zero flow from the piston, the motor tries to maintain a constant speed by drawing oil from the accumulator. Therefore, the accumulator volume and pressure fall during this period, causing the motor speed to reduce as well.
- 13. The accumulator then re-charges when there is maximum flow from the piston as there is more flow than is required by the motor during this time.
- 14. This repeating cycle causes the oscillations in the motor speed, accumulator pressure, and accumulator volume around an average value.

It can be clearly seen that the system does not absorb energy in the same sinusoidal manner as a viscous damper. The force from the piston resembles a square wave so the behaviour is more like that of a Coulomb damper.

3.3 Optimization method

If the PTO unit behaves like a linear viscous damper, it has been shown that there is an optimum damping condition which maximizes the energy absorption. Therefore, even though the hydraulic PTO unit does not absorb energy in the same manner, it is still reasonable to assume that a similar optimum condition to maximize the power produced could be found by altering the effective damping of the hydraulic PTO unit.

Referring the generator characteristic to the piston, the following 'effective damping' term, α , can be

formulated with the same units as a linear viscous damping coefficient

$$\alpha = \left(\frac{A_{\rm p}}{D_{\rm m}}\right)^2 C_{\rm g} \tag{35}$$

To change α , any of the three components can be varied in size; the piston area $(A_{\rm p})$, the motor displacement $(D_{\rm m})$, or the damping coefficient of the generator $(C_{\rm g})$. However, for the purpose of this study, only the motor displacement will be varied, as in practice, it is the easiest of the three components to vary. This means that the variation of $D_{\rm m}$ is being expressed in the form of α in this study. Varying this effective damping will alter the power absorption by varying the pressure in the two accumulators and hence change the force acting on the buoy from the PTO unit.

3.4 Optimization results

When regular monochromatic waves are used as the input to the system, a pseudo steady state condition is reached where the angular velocity and torque produced by the motor oscillates about an average value, as shown in Fig. 7. The amplitude of this oscillation is dependent on the size of the accumulators. In this study, the result presented will be the average value.

To determine if the power produced by the PTO unit can be maximized by changing α , simulations were run with a regular monochromatic wave input of 1 m amplitude for four different wave periods. Figure 10 shows that the power produced by the PTO unit can be maximized by changing α but that

the optimum values of effective damping, $\alpha_{\rm opt}$, are dependent on the wave period. Furthermore, it can be seen that the maximum power which can be produced shows a reduction with increased wave period in this range.

The power of the incident wave is proportional to the square of the wave height [17]; so, if the system was fully linear, this relationship would also hold true for the mechanical power produced by the PTO unit. Simulations were, therefore, run to investigate this theory for a wave period of 10 s with three different amplitudes. Figure 11 clearly shows that at larger wave heights, the value of mechanical power normalized by the square wave amplitude reduces, which

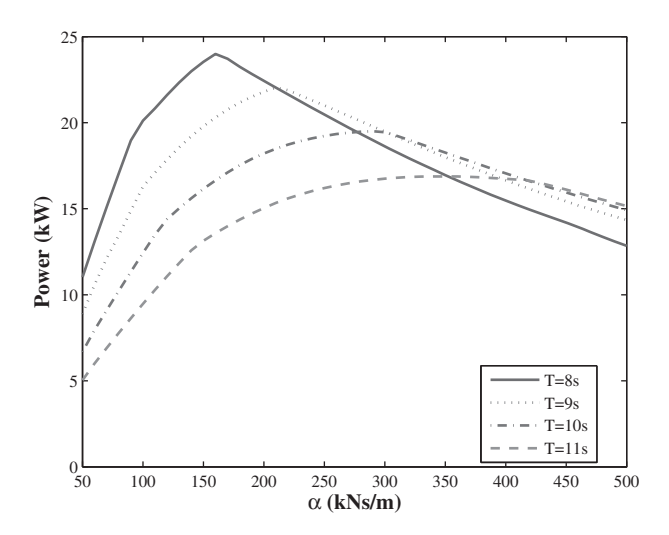


Fig. 10 Mechanical power against effective damping for varying wave periods for a wave height of 2 m

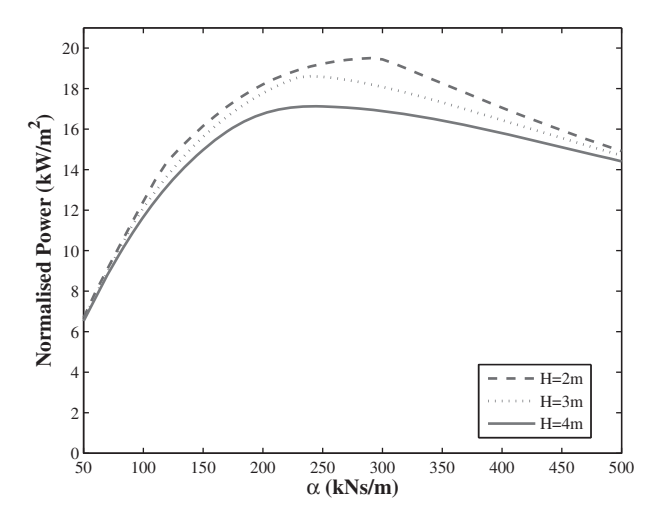


Fig. 11 Normalized mechanical power produced against effective damping for varying wave heights for a wave period of 10 s

indicates that, as expected, the system is non-linear. However, for optimization trends, Fig. 11 also shows a minimal variation in $\alpha_{\rm opt}$ when the wave height is varied for the same wave period.

Therefore, the two trends found from Figs 10 and 11 are that the optimum damping, $\alpha_{\rm opt}$, is highly dependent on wave period but shows little variation with wave height. This follows the linear theory for a viscous damper, but it remains to be found if the values of optimum damping are the same for the different cases

It has been shown already that the hydraulic PTO unit does not absorb energy in the same manner as a viscous damper. Therefore, it is necessary to determine if the theory derived to optimize a linear viscous damper PTO can be applied with confidence to a hydraulic PTO unit. To compare both cases, α is varied to find the power maxima over a range of wave periods. At each power maximum, Φ and α are calculated to discover how these values compare to the values calculated for a viscous damper.

In Fig. 12, the maximum power output against wave period is plotted for a viscous damper and an ideal hydraulic PTO unit with optimal damping values for both cases. It is observed that the maximum power produced by the ideal hydraulic PTO is higher, across this range of wave periods, compared to a viscous damper. However, the difference in power decreases as the wave period increases. As the wave period increases, the wave excitation force also increases, which causes a pressure increase in the accumulator. This, in turn, increases the PTO force, which means that the buoy is arrested for a longer time at its endpoints and so the buoy

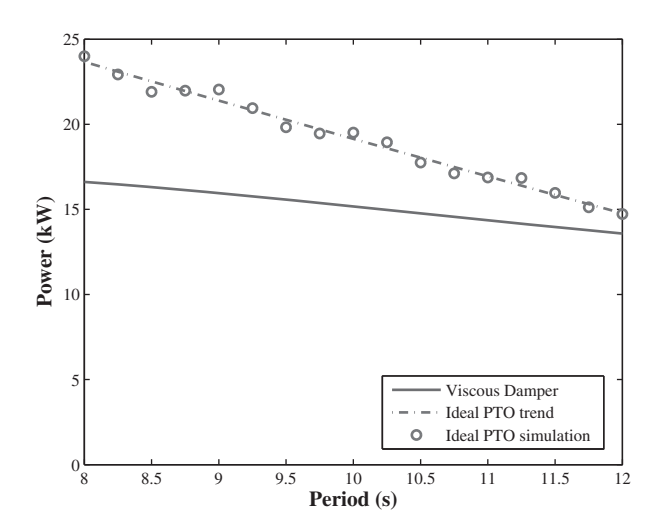


Fig. 12 Maximum mechanical power produced against wave period for an ideal hydraulic PTO and a viscous damper PTO for a wave height of 2 m

displacement is reduced. This causes a lower flow from the cylinder over one cycle and therefore a power reduction from the motor.

Figure 13 shows the comparison between the values of optimum damping for a hydraulic PTO, $\alpha_{\rm opt}$, and those for the linear case of a viscous damper, $C_{\rm opt}$. The viscous damper and the trend for the hydraulic PTO, both show a linear relationship to wave period, but the magnitude of the values is markedly different, which further demonstrates the difference between a viscous damper and a hydraulic PTO.

Another comparison to consider is the optimum PTO force amplitude, $\Phi_{\rm opt}$, for both cases. It is clear from Fig. 14 that the trendline of $\Phi_{\rm opt}$ for a hydraulic PTO unit shows a strong correlation to the values derived for a viscous damper over this range of

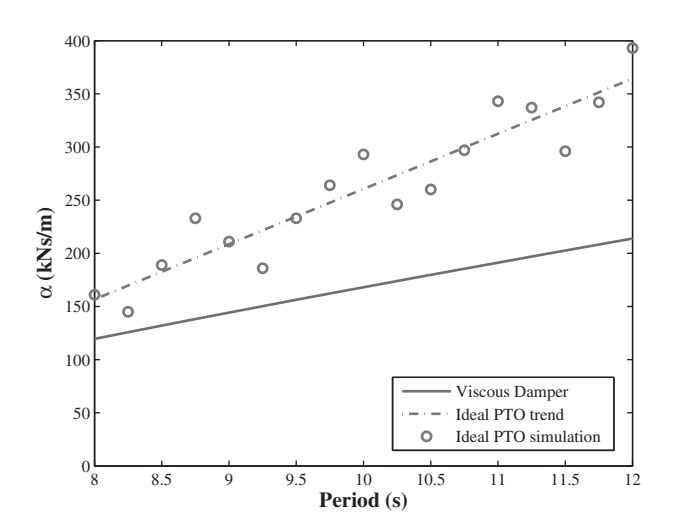


Fig. 13 Optimum damping against wave period for an ideal hydraulic PTO and a viscous damper PTO for a wave height of 2 m

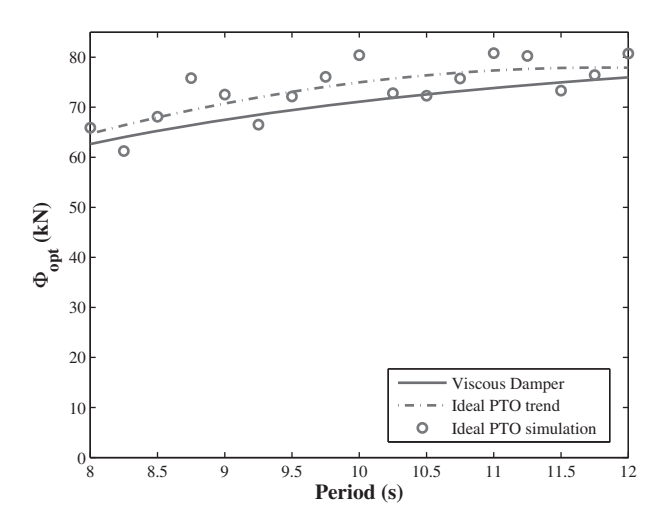


Fig. 14 Optimum PTO force amplitude against wave period for an ideal hydraulic PTO and a viscous damper PTO for a wave height of 2 m

wave periods. This implies that there is an optimum PTO force amplitude, which remains similar irrespective of the type of PTO unit used.

4 HYDRAULIC PTO UNIT INCLUDING LOSSES

To determine more accurately what magnitude of power can be produced from this PTO unit, it is necessary to include losses in the model. This will also show whether the trends previously found to optimize an ideal hydraulic PTO unit still hold true when losses are included. The losses now included in the hydraulic unit are:

- (a) friction in the cylinder;
- (b) friction in the pipework;
- (c) pressure loss across the check valves;
- (d) internal flow leakage in the motor;
- (e) viscous and coulomb friction torque losses in the motor.

The cylinder friction simulates the friction between both piston and piston rod and the cylinder body and is the sum of the coulomb and viscous components. The pressure losses in the pipework are calculated for a fully developed flow, q, and the pressure drop, Δp , across the check valve is obtained with the orifice equation for turbulent flow

$$q = KA_{\rm v} \sqrt{\frac{2\Delta p}{\rho_{\rm o}}} \tag{36}$$

where A_v is the valve area and ρ_o is the oil density. The motor losses have been approximated using the Wilson [18] model with three dimensionless coefficients: the slip coefficient (C_s), the viscous friction coefficient (C_v), and the Coulomb friction coefficient (C_f). The motor torque and flowrate are thus given by

$$T_{\rm m} = (1 - C_{\rm f})D_{\rm m}(p_{\rm a} - p_{\rm b}) - C_{\rm v}D_{\rm m}\mu\omega_{\rm m}$$
 (37)

$$Q_{\rm m} - \frac{C_{\rm s} D_{\rm m} (p_{\rm a} - p_{\rm b})}{\mu} = D_{\rm m} \omega_{\rm m}$$
 (38)

where μ is the dynamic viscosity of the oil. The generator and grid connection losses have not been incorporated at this stage as the main focus of this article is on the hydraulic transmission. Table 2 presents the size and loss coefficients of the components in the circuit.

Initially, to show the reduction in power as a result of the losses in the PTO unit, a simulation was run to compare the two models. The wave conditions and component sizes in the PTO unit remained constant (Table 1) with $D_m = 0.1 \, \text{L/rev}$. The PTO unit efficiency is the ratio of the power generated by the unit to the buoy capture power. There is also the ratio of the buoy capture power to the incident wave power,

which is defined as the buoy capture efficiency. These two terms are combined to give the overall WEC efficiency.

With PTO unit losses included, the buoy capture efficiency is lower compared to the case of the ideal PTO unit, indicating that the inclusion of losses causes the overall device to behave differently. It can be seen from Table 3 that even for a wave height of 2 m, there is still a significant power loss of 4.32 kW from the PTO unit, giving a PTO unit efficiency of approximately 80 per cent. To identify where the biggest losses occur in the PTO unit, the power loss from each of the components is presented in Table 4, which indicates that the motor is the main contributor to power loss in the circuit. Hydraulic motors have an optimum speed to pressure ratio, which maximizes the overall efficiency of the motor and it is important to be working close to this value. Therefore, this loss will depend on the specific operating point of the motor, which will vary depending on the wave conditions.

There is also a significant loss from the friction in the cylinder and the pressure drop across the check valves. The viscous component of the cylinder friction will increase with buoy velocity and the pressure

Table 2 PTO unit component loss parameters

Cylinder	
Coulomb friction	$3.5\mathrm{kN}$
Viscous friction	0.1 kN/(m/s)
Variable displacement motor	
$C_{\rm s}$	2×10^{-9}
$C_{\rm v}$	2×10^{5}
$C_{ m f}$	0.03
Check valve	
Maximum area	$250\mathrm{mm}^2$
Flow discharge coefficient	0.7
Cracking pressure	0.3 bar
Pipework	
Diameter	50 mm
Total length	20 m
5	

Table 3 Power loss for a wave height of 2 m and period of 8 s

Wave power	125 kW
Buoy capture power	21.44 kW
Power generated	17.12 kW
Power loss in PTO unit	4.32 kW
Buoy capture efficiency	17.2%
PTO unit efficiency	79.9%
WEC efficiency	13.7%

Table 4 Power loss in the hydraulic circuit

Power loss (kW)	
Cylinder	1.14
Check valves	1.42
Pipework	0.06
Motor	1.70

drop is similar to a viscous friction effect, so it will increase when piston velocity and flows increase at larger wave heights. To minimize this pressure drop, the flowrate in the circuit could be reduced using a smaller piston area. However, this approach must be matched by the requirement to choose a piston area which is still large enough so as to not violate the maximum system pressure when the piston is working at its stroke limit.

Figure 15 shows the PTO unit efficiency over a range of wave heights for a wave period of 8 s. It indicates, however, that the PTO unit efficiency only reduces slightly at large wave heights due to a number of reasons. First, the cylinder friction is Coulomb dominant and so the overall loss from the cylinder does not increase greatly with wave height. Second, the motor efficiency remains approximately constant for all wave heights as the relationship between pressure differential across the motor and motor speed remains almost constant. However, as expected, the pressure drop across the check valves increases exponentially with wave height, which produces the slightly reduced overall unit efficiency.

4.1 Optimization results

The final part of this study compares the optimization results for an idealized PTO unit with the results for a realistic PTO with losses. Therefore, the same simulations were run with the motor displacement, $D_{\rm m}$, being varied to alter the effective damping of the PTO, α .

Figure 16 shows the result that is equivalent to that in Fig. 11. It is clear that the maximum mechanical power normalized by the square wave amplitude is lower than before at each wave height. Furthermore,

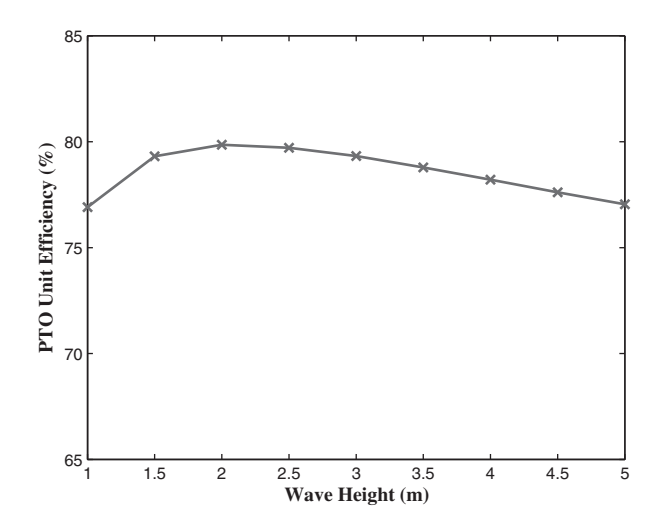


Fig. 15 PTO unit efficiency against wave height for a wave period of 8 s and $D_{\rm m}$ = 0.1 L/rev

it is noted that this reduction increases with wave height due to a reduced buoy capture efficiency and a reduction in PTO unit efficiency, for the reasons previously discussed. However, in relation to optimization trends, Fig. 16 shows that $\alpha_{\rm opt}$ does not change with wave height for the same wave period. This is the same trend as before and the values of $\alpha_{\rm opt}$ are similar to Figure 11.

The similarity between the values of optimum damping for a hydraulic PTO unit with losses and an ideal PTO unit are shown in Fig. 17. It can be seen that both cases produce a near identical linear trend line of optimum damping against wave period, which is encouraging as it allows these devices to be

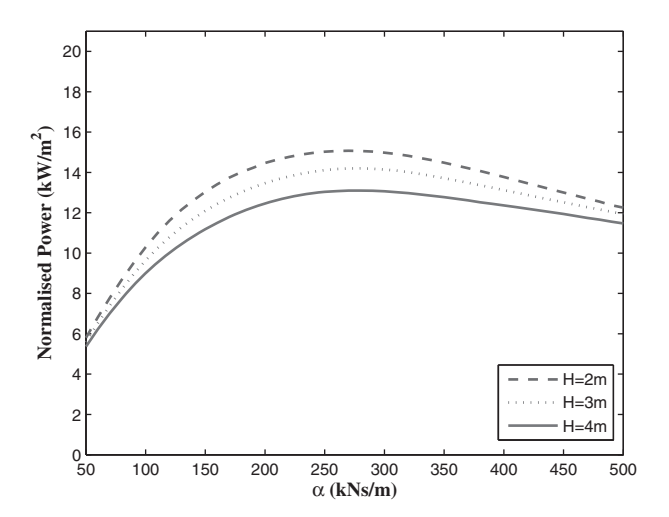


Fig. 16 Normalized mechanical power produced against PTO effective damping for varying wave height for a wave period of 10 s with losses included

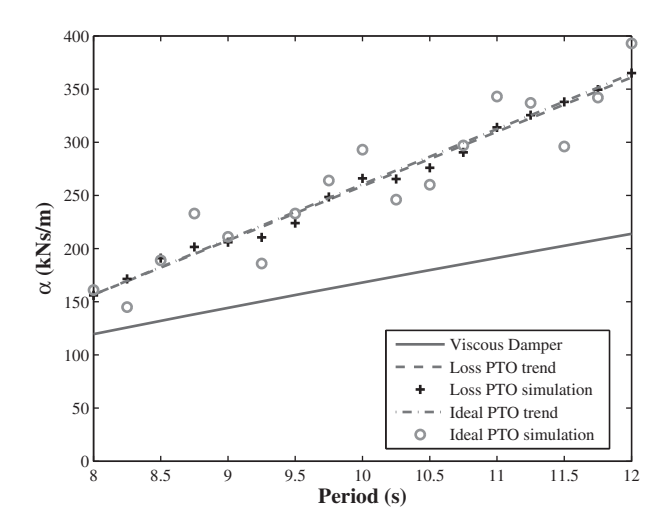


Fig. 17 Optimum damping against wave period for an ideal hydraulic PTO, a hydraulic PTO with losses, and a viscous damper PTO for a wave height of 2 m

optimized using the simpler model of the ideal PTO unit. However, neither case is comparable to a viscous damper, indicating that the hydraulic PTO unit absorbs energy in a different manner.

It is important to discover the reduction in power produced when losses are included in the PTO unit. Figure 18 shows that, in this range of wave periods, the power produced from the PTO unit including losses follows a similar trend to the ideal PTO unit. For this wave height, the PTO unit shows an efficiency of between 79 and 82 per cent, for the optimal case, with efficiency slightly increasing with wave period due to the reduced buoy velocity. It is also noted that the PTO unit with losses included shows a higher maximum power than the case of a viscous damper over part of the range of wave periods. This is encouraging as it could be assumed that an ideal viscous damper would produce a substantially larger power over the full range of wave periods.

It has been shown that the values of optimum damping are not related to those for a viscous damper. However, for the values of optimum PTO force amplitude, $\Phi_{\rm opt}$, Fig. 19 indicates that the trend line for the PTO unit including losses shows a strong correlation to the trend line for the ideal PTO unit and the case of a viscous damper. This indicates that irrespective of how the device absorbs energy, there is an optimum force which the PTO unit should produce to maximize the power output. This implies that the device could be optimized by ensuring the hydraulic PTO unit produces a specific force, which could be calculated from the theory for a simple viscous damper, by varying the effective damping of the PTO unit.

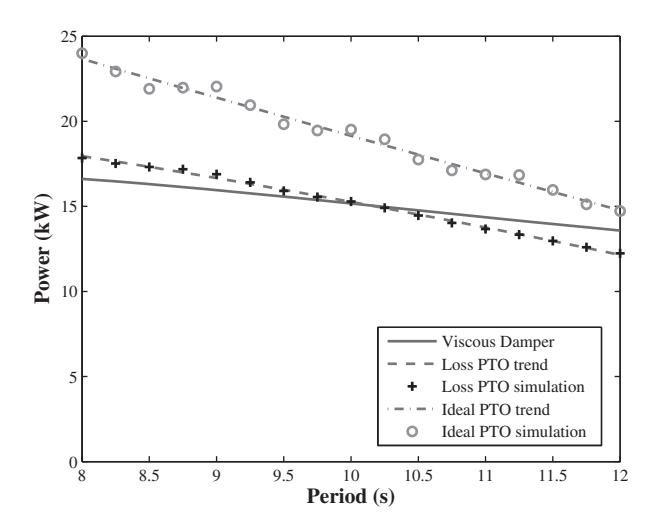


Fig. 18 Maximum mechanical power produced against wave period for an ideal hydraulic PTO, a hydraulic PTO with losses, and a viscous damper PTO for a wave height of 2 m

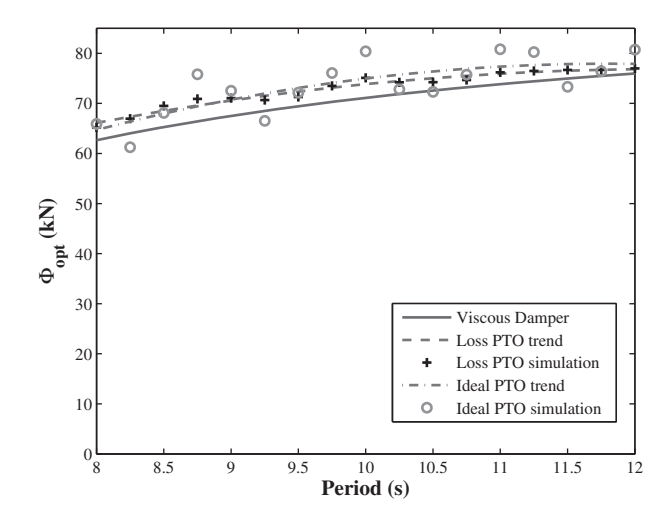


Fig. 19 Optimum PTO force amplitude against wave period for an ideal hydraulic PTO, a hydraulic PTO with losses, and a viscous damper PTO for a wave height of 2 m

5 CONCLUSION

This study has described a time domain analysis of a floating buoy, oscillating in heave with a hydraulic PTO unit in regular monochromatic waves. It is fully understood that monochromatic sea waves do not occur in reality but it is useful to fully comprehend the operation of these complex WEC devices in regular waves before they can be investigated under more realistic conditions.

It has been shown that a typical hydraulic PTO unit behaves similar to a Coulomb damper producing a square wave force rather than the sinusoidal nature of a viscous damper as previously assumed. The hydraulic PTO unit was modelled as both an ideal unit and a unit including losses so that a realistic power output and PTO unit efficiency could be predicted. The PTO unit efficiency was found to only vary slightly with wave height.

It has been shown that a hydraulic PTO unit can be optimized, in the same manner as a viscous damper, by altering the motor displacement, which varies the effective damping of the unit. The optimum damping of the PTO unit has a linear relationship to wave period but only a minimal variation with wave height. The inclusion of losses in the model has no effect on the optimum values for the effective damping of the PTO unit. The optimum value is not the same as that of a viscous damper.

However, all three cases investigated showed a similar trend for the optimum PTO force amplitude against wave period. This implies that for a given wave period, regardless of PTO design, there is an optimum force amplitude which the PTO unit should produce to maximize the power generated.

Hence, the next stage of study will be to investigate a force control strategy and develop a control algorithm to optimize the device in varying sea conditions. Furthermore, it will be necessary to investigate the response of the device in irregular waves and determine whether similar optimum conditions and trends exist.

© Authors 2011

REFERENCES

- 1 Cruz, J. (Ed.) Ocean wave energy: current status and future perspectives, 2008 (Springer, Berlin, Germany).
- **2 Drew, B., Plummer, A. R.,** and **Sahinkaya, M. N.** A review of wave energy converter technology. *Proc. IMechE, Part A: J. Power and Energy,* 2009, **223**(8), 887–902.
- **3 Henderson, R.** Design, simulation, and testing of a novel hydraulic power take-off system for the Pelamis wave energy converter. *Renewable Energy*, 2006, **31**(2), 271–283.
- **4 Falcão, A. F. de O.** Wave energy utilization: a review of the technologies. *Renewable Sustainable Energy Rev.*, 2010, **14**, 899–918.
- 5 Rahm, M., Boström, C., Svensson, O., Grabbe, M., Bülow, F., and Leijon, M. Offshore underwater substation for wave energy conerter arrays. *Renewable Power Gener.*, 2010, 4, 602–612.
- **6 Plummer, A. R.** and **Schlotter, M.** Investigating the performance of a hydraulic power take-off. In Proceedings of the 8th European *Wave and tidal energy conference*, Uppsala, Sweden, 7–10 September 2009.
- **7 Falcão, A. F. O.** Modelling and control of oscillating-body wave energy converters with hydraulic power take-off and gas accumulator. *Ocean Eng.*, 2007, **34**, 2021–2032.
- **8 Falcão, A. F. O.** Phase control through load control of oscillating-body wave energy converters with hydraulic PTO system. *Ocean Eng.*, 2008, **35**, 358–366.
- **9 Babarit, A., Duclos, G.,** and **Clément, A. H.** Comparison of latching control strategies for a heaving wave energy device in random sea. *Appl. Ocean Res.*, 2005, **26**(5), 227–238.
- **10** Yavuz, H., McCabe, A., Aggidis, G., and Widden, M. B. Calculation of the performance of resonant wave energy converters in real seas. *Proc. IMechE, Part M: J. Engineering for the Maritime Environment*, 2006, **220**(3), 117–128.
- 11 Yavuz, H., Stallard, T. J., McCabe, A. P., and Aggidis, G. Time series analysis-based adaptive tuning techniques for a heaving wave energy converter in irregular seas. *Proc. IMechE, Part A: J. Power and Energy*, 2007, 221(1), 77–90.
- **12 Folley, M.** and **Whittaker, T.** The control of wave energy converters using active bipolar damping. *Proc. IMechE, Part M: J. Engineering for the Maritime Environment,* 2009, **223**(4), 479–487.
- **13 Babarit, A., Guglielmi, M.,** and **Clément, A. H.** Declutching control of a wave energy converter. *Ocean Eng.*, 2009, **36**, 1015–1024.

K

L

m

p

 p_i

 p_o

 \bar{P}

 $P_{\rm m}$

q

 q_i

 $q_{\rm m}$

S t flow coefficient

mass of buoy

average power

mechanical power

accumulators i = A, B flowrate to the motor

buoy cross-sectional area

accumulators i = A, B

initial accumulator pressure

pressure

flowrate

time

radiation impulse response function

pressure in piston chambers i=1, 2 and

flowrate in check valves i = 1, 2, 3, 4 and

14	Falnes, J. Ocean waves and oscillating systems, 2	002
	(Cambridge University Press, Cambridge, UK).	

- 15 Eriksson, M., Isberg, J., and Leijon, M. Hydrodynamic modelling of a direct drive wave energy converter. Int. J. Eng. Sci., 2005, 43, 1377-1387.
- 16 Cummins, W. E. The impulse response function and ship motions. Schiffstechnik, 1962, 9, 101-109.
- 17 McCormick, M. Ocean wave energy conversion, 1981 (Wiley, New York).
- 18 Wilson, W. E. Performance criteria for positive displacement pumps and fluid motors. Trans. Am. Soc. Mech. Eng., 1949, 71(2).

APPENDIX

Notation

Notation		•		
		$T_{ m g}$	generator torque	
	$A(\omega)$	frequency-dependent added mass	$T_{ m m}$	motor torque
	A_{∞}	added mass at infinite frequency	$U(j\omega)$	velocity in the frequency domain
	$A_{\rm p}$	piston area	$U_{ m opt}$	optimum buoy velocity
	$A_{ m v}$	valve area	V_i	oil volume in piston chambers $i=1, 2$ and
	B	oil bulk modulus		accumulators $i=A$, B
	$B(\omega)$	frequency dependent radiation damping	$V_{ m o}$	initial oil volume in accumulators
		coefficient	$\boldsymbol{\mathcal{X}}$	buoy displacement
	C	viscous damper coefficient	\dot{x}	buoy velocity
	$C_{ m f}$	Coulomb friction coefficient of motor	\ddot{x}	buoy acceleration
	$C_{\rm g}$	generator damping coefficient	X(s)	Laplace transform of position, $x(t)$
	$C_{ m opt}$	optimum viscous damper coefficient		
	$C_{\rm s}$	slip coefficient of motor	α	effective PTO damping
	$C_{\rm v}$	viscous friction coefficient of motor	$\alpha_{ m opt}$	optimum effective PTO damping
	$D_{ m m}$	motor displacement	γ	adiabatic index
	$f_{ m e}$	wave excitation force	$\Gamma(\omega)$	wave excitation force coefficient
	$f_{ m h}$	wave force	μ	oil dynamic viscosity
	$f_{ m hs}$	wave hydrostatic force	ρ	water density
	$f_{ m m}$	mechanical force	$ ho_{ m o}$	oil density
	$f_{ m r}$	wave radiation force	τ	dummy time variable
	$F_{\rm e}(s)$	Laplace transform of wave excitation force	Φ	PTO force
	g	gravitational acceleration	Φ_{opt}	optimum PTO force
	H	wave height	ω	wave frequency
	j	imaginary unit, $\sqrt{-1}$	$\omega_{ m m}$	angular velocity of the motor
	J	generator inertia		